Thermodynamic Modeling of an Ammonia-Water Absorption System Associated with a Microturbine

Janilson Arcangelo Rossa and Edson Bazzo[1*]

Federal University of Santa Catarina, Department of Mechanical Engineering, Florianópolis, Brazil

E-mail: [1]ebazzo@emc.ufsc.br

Abstract

Thermodynamic modeling and Second Law analysis of a small-scale cogeneration system consisting of a 5 refrigerant ton absorption chiller connected by a thermosyphon heat exchanger to a 28 kW$_e$ natural gas microturbine are presented. The proposed configuration changes the heat source of the absorption chiller, replacing the original natural gas burning system. A computational algorithm was programmed to analyze the global efficiency of the combined cooling and power plant and the coefficient of performance of the absorption chiller. The results show the consistency of the proposed model and a good performance of the cogeneration system. The thermal efficiency of the combined cooling and power plant is approximately 41%, which represents a 67% increase relative to a single natural-gas microturbine.

Keywords: Cogeneration, natural gas microturbine, ammonia-water absorption chiller, second law analysis.

1. Introduction

Absorption refrigeration can become economically attractive when using inexpensive heat energy at temperatures in the range of 100 to 300ºC. However the absorption refrigeration technology has been constrained to large commercial and industrial installations, where a large amount of thermal energy is required. For cost reasons, the most frequently used refrigeration cycle has been the vapor-compression refrigeration cycle. During recent years, the increasing accessibility to natural gas and the continuously increasing costs of energy have recommended the use of new technologies or the use of high-efficiency equipment in cogeneration systems for power, steam, hot water or cold water generation. In this new scenario, absorption chillers are proposed here to be used also in small-scale plants based on natural gas microturbines, for power and cold water generation.

Recent results from experimental and theoretical investigations (Medrano *et al.*, 2006; Takeshita *et al.*, 2005; Rucker *et al.*, 2004 and Rucker *et al.*, 2003) have been reported in order to confirm the plant operation reliability and to show the high global performance of small-scale cogeneration systems using absorption chillers. In this work, a thermodynamic model is presented for a small-scale cogeneration plant with simultaneous production of power and cold water. The small-scale plant consists of a 5 refrigerant ton (RT) ammonia-water refrigeration system connected to a 28 kW$_e$ microturbine, both driven originally by natural gas. The ammonia-water cycle was selected because it does not crystallize when submitted to elevated temperatures, as happens with the water-LiBr cycle. The proposed configuration changes the heat source of the chiller, replacing the natural gas burning system with a heat exchanger connected to a microturbine. The exhaust gas coming from the microturbine, when entering the heat exchanger, warms the ammonia-water solution and drives the ammonia separation in the chiller. The ammonia-water solution flow between the heat exchanger and the generator is established by the thermosyphon effect. No secondary thermal fluid was proposed to transfer the residual energy

from the exhaust gas to the generator. The thermodynamic simulation takes into account environmental changes. The results show the reliability and good performance of the proposed configuration under different operating conditions. The corresponding values are used to analyze the operation parameters' influence on the coefficient of performance (COP), the microturbine efficiency and especially on the global efficiency or primary energy ratio of the cogeneration system. A Second Law analysis was considered to quantify the irreversibility of each chiller component and also to determine the potential of each component that contributes to the energy savings.

2. System description

The small-scale cogeneration system consists of a 5 RT Robur gas fired chiller of single effect (17.7 kW), connected to a 28 kW$_e$ Capstone turbine model C30 LP by a thermosyphon heat exchanger. The residual energy of the exhaust gas is recovered for driving the absorption chiller before it is discharged to the environment. In Figure 1 the schematic of the cogeneration system with four subsystems is shown including the natural gas supply, microturbine, heat recovery and absorption chiller. The technical specifications of the natural gas microturbine and the absorption chiller, used for setting the computational code, are shown in Table 1.

As shown in Figure 1, natural gas is supplied to the microturbine to produce electricity and hot exhaust gas for the heat exchanger. The pressure of the supplied natural gas is 150 kPa (1.5 bar) and the temperature of the hot exhaust gas is about 260 °C. An existing internal fuel-gas compressor increases the natural gas pressure from 359 to 379 kPa. An external pressure regulator is used to maintain a steady fuel pressure at the microturbine inlet in order to limit pressure oscillations within ±7 kPa.

The exhaust gas from the microturbine is passed through the proposed thermosyphon heat exchanger. The heat is directly transferred to the ammonia-water solution. No intermediate fluid is used that would increase the thermal resistance.

*Corresponding Author

Microturbine	
Output power	28 kW
Efficiency	26%
Fuel	Natural Gas
Exhaust gas temp.	270 °C
Exhaust gas flow rate (SCG*)	17 Nm³/min

Absorption Chiller	
Cooling capacity	17.7 kW
COP	0.6
Min. chilled water temp.	+4 °C
Max. environment temp.	55 °C
Nominal air flow rate (SCG*)	10 Nm³/h

*Nm³ is m³ at SCG – Standard Conditions for Gases (T=0°C and P=101.325 kPa)

A solution of water and ammonia is used as the working fluid, where ammonia is the refrigerant and water is the absorbing fluid. In the proposed heat exchanger, the ammonia-water is heated to boiling, producing vapor with a strong concentration of ammonia, and as a consequence, a liquid solution with a weak concentration of ammonia.

A thermosyphon effect was considered to provide the circulation of the water-ammonia solution from the generator through the heat exchanger. The thermosyphon system has the advantage of providing direct heating and avoids the use of an expensive circulation pump. Nevertheless, for effective operation of the system the heat exchanger must be positioned below the absorption chiller to allow the vapor ammonia to return to the generator. One of the first thermosyphon applications is a Perkins tube, which uses a two-phase process to transfer heat from a furnace to a boiler (Dunn, 1997; Peterson, 1994).

The ammonia vapor flows into the rectifier for purification. The hot and pressurized ammonia vapor exiting the rectifier enters the air-cooled condenser where it is cooled and condensed.

The liquid ammonia is then brought to a lower pressure (assumed 1536 kPa) by means of an initial expansion valve after which it is cooled in a pre-cooler. Finally, the liquid ammonia pressure is again reduced by a second expansion valve from 1536 kPa to an absolute pressure of 458 kPa and temperature of approximately 2 °C. At this condition, the liquid ammonia enters the evaporator and produces chilled water to meet the cooling demand.

A vapor-liquid mixture of ammonia leaves the evaporator at 4 °C, flowing again through the pre-cooler where it cools the liquid ammonia coming from the air condenser. The ammonia vapor enters the absorber and comes into direct contact and subsequent dilution with the weak solution coming from the generator through a third expansion valve. The absorption of ammonia vapor is an exothermic process.

The solution flows from the absorber to a subsequent section of the heat exchanger near the air condenser for cooling and complete absorption. The lower the temperature, the higher the ammonia concentration. At this point, the liquid solution with a high concentration of ammonia (strong solution) is pumped through a coil inside the rectifier and through another coil inside the absorber (GAX system) back to the generator. A hydraulically driven diaphragm pump is used to displace the strong solution to the high pressure level in the generator.
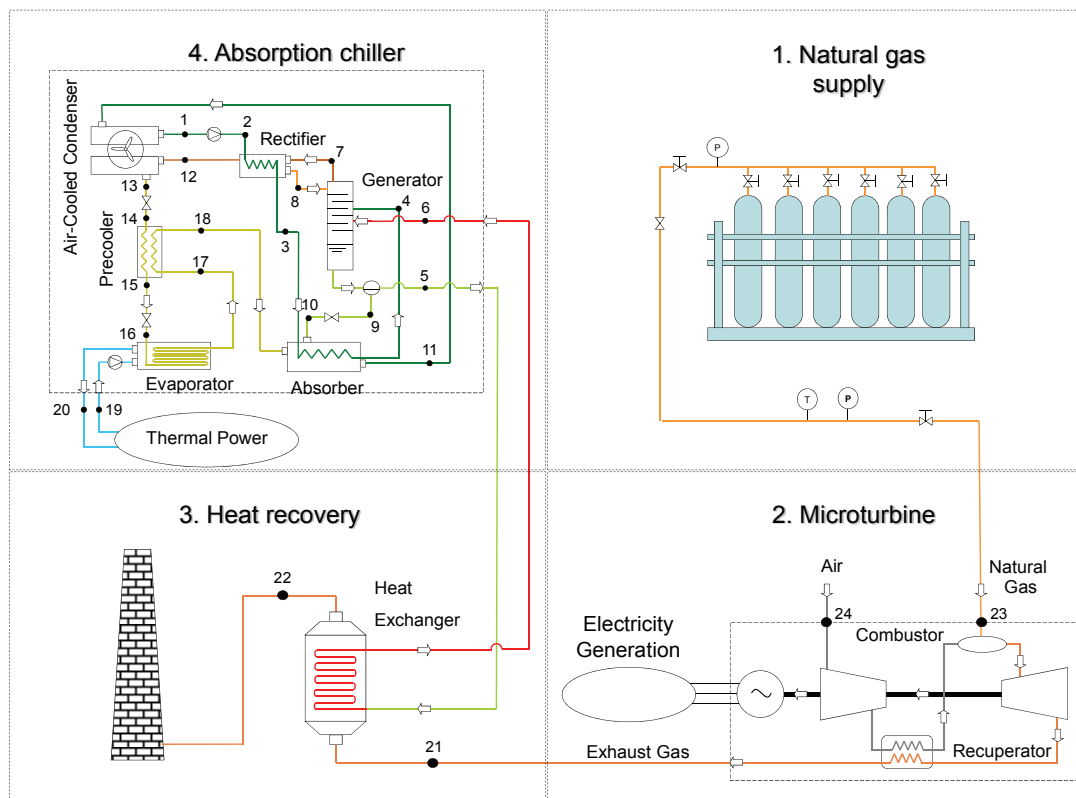

Figure 1. Schematic Diagram of the Cogeneration System.

3. Thermodynamic analysis

The principle of mass conservation and the First and Second Laws of Thermodynamics were applied to each component of the system for the analysis. Every component was considered as a control volume, taking into account the heat transfer, work interaction and inlet and outlet streams. The microturbine was not modeled at the same level of detail as the absorption chiller, since it is not the focal point of this work. The governing equations for mass conservation are:

$$\sum \dot{m}_i - \sum \dot{m}_o = 0 \tag{1}$$

$$\sum \dot{m}_i x_i - \sum \dot{m}_o x_o = 0 \tag{2}$$

where x_i and x_o correspond to the inlet and outlet ammonia mass fractions.

The First Law of Thermodynamics yields the energy balance of each component of the whole system in following form

$$\dot{Q} - \dot{W} = \sum \dot{m}_o h_o - \sum \dot{m}_i h_i \tag{3}$$

and subjected to the following assumptions:

- Steady state operation;
- Thermodynamic equilibrium at all points;
- Output power equal to 26 kWe;
- Inlet temperature of the generator: $T_6 = 120ºC$;
- Refrigerant vapor concentration leaving the rectifier equal to 0.99 (point 12);
- Difference between inlet and outlet chilled water temperatures equal to 5°C;
- Environmental condition of 25°C;
- Dead state of 25°C and 101.325 kPa.

The refrigerant vapor concentration was set equal to 0.99 and variations with operating conditions were neglected.

Only the residual energy from the microturbine exhaust gas was considered as the energy source of the heat exchanger. A minimum inlet temperature of the generator of $T_6 = 120ºC$ (see Figure 1) was considered for the simulation. The vapor mass flow rate at point 7 was correlated to the vapor mass flow rate generated inside the heat exchanger.

The *COP* of the absorption system is defined as:

$$COP = \frac{\dot{Q}_{cool}}{\dot{m}_{21} \cdot c_{p,e} \left(T_{21} - T_{ref} \right)} \tag{4}$$

where $\dot{Q}_{cool}$ is the cooling load met by the evaporator (see Figure 1) and the corresponding denominator represents the available energy associated with the microturbine exhaust gas entering the heat exchanger. This COP includes the heat exchanger as part of the absorption chiller.

As used in the COP calculation for an absorption chiller using a direct firing system, the COP, evaluated in equation (4), is based on the effective available energy in the exhaust gas. The T_{ref} considered here is 25 ºC, the same reference temperature for the Lower Heating Value (LHV) of the fuels. In fact, for both cases, it is impossible to cool the gas to the reference temperature.

The global efficiency, or primary energy ratio, of the combined cooling and power (CCP) system is defined as

$$\eta_{CCP} = \frac{\dot{W}_e + \dot{Q}_{cool}}{\dot{Q}_{fuel}} \tag{5}$$

where $\dot{W}_e$ is the power output of the microturbine, $\dot{Q}_{cool}$ is again the cooling load met by the evaporator and $\dot{Q}_{fuel}$ is the fuel energy required by the microturbine.

The Second Law of Thermodynamics was used for analysis and calculation of the CCP performance based on exergy. Disregarding magnetic, electrical, nuclear, and surface tension effects, the total exergy of the system becomes the summation of physical and chemical exergies as

$$\psi = \psi^{ch} + \psi^{ph} \tag{6}$$

The physical exergy of a fluid stream is defined as:

$$\psi^{ph} = \left(h - h_0 \right) - T_0 \left(s - s_0 \right) \tag{7}$$

where h and s are the enthalpy and the entropy of the fluid, respectively.

The calculation procedure for the chemical exergy of various substances based on standard chemical exergy values has been widely discussed in Szargut *at al.* (1988). For the water-ammonia solution considered here, the chemical exergy of the flows was approximated using the following expression:

$$\psi^{ch} = \frac{x}{M_{NH_3}} e^0_{ch,NH_3} + \frac{(1-x)}{M_{H_2O}} e^0_{ch,H_2O} \tag{8}$$

where e^0_{ch,NH_3} and e^0_{ch,H_2O} are the chemical exergies of ammonia and water, respectively, as given by Ahrendts (1980). The chemical exergy unit is kJ/kmol. The exergy destroyed in each component was calculated as

$$\dot{X}_{des} = \sum \dot{m}_i \psi_i - \sum \dot{m}_o \psi_o + \sum \dot{Q} \left(1 - \frac{T_0}{T} \right) - \dot{W} \tag{9}$$

where the first two terms of the right hand side are the inlet and outlet exergy streams of the control volume. The third term is associated with the exergy of heat transferred from the source at temperature T. The last term is the exergy of the mechanical work.

The total destroyed exergy of the absorption system is the sum of destroyed exergies for each component:

$$\dot{X}_{des}^{Total} = \sum \dot{X}_{des}^k \tag{10}$$

The Second Law efficiency of the system is measured by the exergy efficiency, defined as the ratio of the useful exergy produced by the system to the fuel exergy supplied to the system. Therefore, the exergy efficiency of the cogeneration system is the sum of the electricity energy generated by the microturbine and the exergy increase of the chilled water in the evaporator divided by the corresponding exergy of the heat source:

$$\varepsilon_{CCP} = \frac{\dot{W}_e + \dot{m}_{20} \left(\psi_{20} - \psi_{19} \right)}{\dot{m}_{fuel} \, \psi_{fuel}} \tag{11}$$

where ψ_{fuel} is the fuel exergy, assumed to be equal to the LHV of the natural gas obtained from the natural gas supplier company - SCGas.

The calculations were carried out using the software EES with the NH$_3$-H$_2$O library. The property routines in the NH$_3$-H$_2$O library used the correlation described by Ibrahim and Klein (1993).

4. Results and discussion

As assumed before, for an output power equal to 26 kW$_e$, the results concerning the performance and exergy destruction are given in Tables 2 and 3, respectively. Other input data include the environmental conditions, natural gas lower heating value, heat exchanger effectiveness, and chilled water flow rate, inlet and outlet temperatures. The values of pressure, temperature, enthalpy, entropy, mass concentration, mass flow rate, and exergy of the solution were calculated. The operating conditions of the whole system are shown in Table 4.

Table 2. Performance Results.

Cogeneration plant	Symbol	Value
Global efficiency	η_{CCP}	41.9 %
Exergy efficiency	ε_{CCP}	25 %
Microturbine		
Efficiency	η_{MT}	25.1 %
Natural gas (SCG)	$\dot{m}_{fuel}$	10.45 Nm³/h
Cooling system		
Coefficient of performance	COP	0.27

As shown in Table 2, the COP was calculated as 0.27, which is at least 50% smaller than the nominal COP for the direct firing system. It is important to emphasize the available energy associated with the exhaust gas entering the heat exchanger and the corresponding temperature reference, as defined by Eq. 4. The exergy efficiency of the plant and the CCP global efficiency were estimated as approximately 25 and 42%, respectively.

Table 3. Exergy Destruction.

Component	$\dot{X}_{des}$ [kW]
Microturbine	41.29
Absorption chiller	37.50
Heat exchanger/Generator	27.87
Absorber	3.65
Expansion valves	1.75
Precooler	1.53
Air Condenser	1.15
Rectifier	1.02
Evaporator	0.49
Hydraulic Pump	0.04

The largest irreversibilities are associated with the fuel combustion for the microturbine and the heat exchanger/generator for the absorption chiller. As expected, the fuel burning in the microturbine causes very large irreversibilities.

In the case of the absorption chiller, a large amount of thermal energy is required in the heat exchanger/generator

to drive the separation of ammonia from the strong solution. The exergy destruction in the absorber takes into account all the irreversibilities related to the absorber itself and the subsequent section of the heat exchanger, placed close to the air condenser. The other components presented relatively low exergy destructions.

As seen in Table 3, the microturbine has the greatest exergy destruction followed by the heat exchanger as a consequence of the heat exchanging or corresponding ammonia-water separation.

Further analysis is now focused on the prediction of system efficiencies for different chilled water temperatures. Figure 2 shows the influence of different chilled water temperatures on the COP and exergy efficiency. The higher the evaporator temperature, the higher the chilled system's COP. This is because the solution concentration difference increases and the solution mass flow rate is reduced. So the heat transferred from the exhaust gas to the ammonia-water solution decreases and the COP increases.

As defined in this work, the COP includes the heat exchanger as part of the absorption chiller and it is referenced to the effective available energy in the exhaust gas, considering T_{ref} equal to 25ºC. Considering the actual heat removed from the microturbine exhaust gas and for the chilled water temperature equal to 5ºC, the COP becomes 0.52.

On the other hand, the CCP exergy efficiency decreases slightly with increasing outlet chilled water temperatures. The exergy efficiency decreases because the exergy of the chilled water decreases with increasing outlet temperature since the chilled water is at a temperature less than the dead state's temperature.
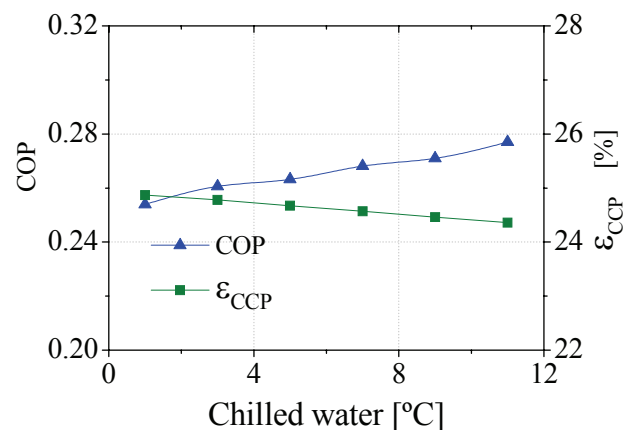

Figure 2. The Effect of Chilled Water Temperature on the COP and CCP Exergy Efficiency.

The general results of the whole system for the temperature, mass fraction of ammonia, pressure, enthalpy, mass flow rate and exergy obtained from the thermodynamic simulation are shown in Table 4.

Figure 3 shows the variation of the CCP global efficiency, microturbine efficiency and CCP exergy efficiency with the plant's power output. As can be seen from the figure, the higher the output power, the higher the CCP global efficiency, the microturbine efficiency, and exergy efficiency. A maximum global efficiency of approximately 42% was found for 25 kW$_e$ output, which represents a 67% efficiency increase relative to a single microturbine power plant.

Table 4. General Results Obtained from the Thermodynamic Simulation.

| Point	Temperature [°C]	x [% NH$_3$]	P [kPa]	h [kJ/kg]	$\dot{m}$ [kg/s]	ψ [kJ/kg]
1	40.0	0.471	458	91.0	0.1392	9390
2	40.2	0.471	1538	92.7	0.1392	9391
3	51.4	0.471	1538	145.0	0.1392	9394
4	88.1	0.471	1538	358.4	0.1392	9424
5	102.3	0.396	1538	394.5	0.1340	7945
6	120.0	0.396	1538	666.2	0.1340	8006
7	115.0	0.920	1538	1905.0	0.0206	18676
8	76.1	0.525	1538	286.1	0.0031	10493
9	102.3	0.396	1538	394.5	0.1217	7945
10	68.5	0.396	458	394.5	0.1217	7931
11	52.5	0.471	458	330.6	0.1392	9405
12	76.1	0.990	1538	1751.0	0.0175	20027
13	40.0	0.990	1538	522.1	0.0175	19956
14	39.9	0.990	1536	522.1	0.0175	19956
15	11.4	0.990	1536	385.0	0.0175	19956
16	2.0	0.990	458	385.0	0.0175	19953
17	4.0	0.990	458	1448.0	0.0175	19866
18	13.0	0.990	458	1585.0	0.0175	19857
19	12.2	-	200	51.5	0.8452	1.279
20	7.2	-	200	30.5	0.8452	2.411
21	251.0	-	102	528.0	0.2797	195.8
22	126.8	-	101	401.3	0.2797	73.4
23	25.0	-	101	-	0.0021	49661
24	25.0	-	101	-	0.2775	49.96
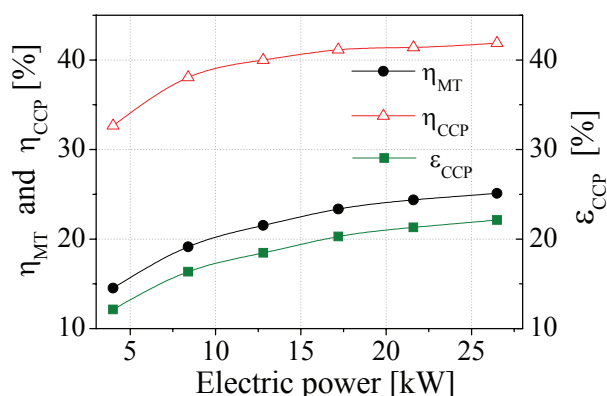
Figure 3. Variation of the Microturbine Efficiency, Global Efficiency and Exergy efficiency with Microturbine Power Output.

The microturbine efficiency decreases with increasing environmental temperature. As a consequence, the exergy efficiency and the global efficiency presented a small decline. In fact, there is no significant change in the exergy destruction in the microturbine and in the chilled system.

5. Conclusions

The absorption chiller connected by a thermosyphon heat exchanger to a microturbine was analyzed as a technically reliable alternative for chilled water and power generation. The results show the consistency and usability of the proposed thermodynamic model.

A CCP global efficiency up to 42% was found, which represents a 67% efficiency increase relative to a single microturbine power plant.

The COP was calculated to be approximately 0.27 (for a chilled water temperature of 5ºC), which is at least 50% smaller than the nominal COP for the direct firing system. As defined before, the COP is referenced to the effective available energy in the exhaust gas (T_{ref} = 25ºC). For a COP referenced to the real heat supplied from the heat exchanger to the generator, the COP is 0.52. The COP increases with increasing chilled water temperature.

The exergy efficiency of the plant was estimated to be approximately 25%. The exergy efficiency decreases slightly with increasing environment temperature. A more sensitive influence on the exergy efficiency has been observed for output power variation than for the variation of the operational parameters of the chiller.

The exergy destruction was calculated for every component of the system. The microturbine presented the highest rate of exergy destruction (approximately 41 kW). In the chiller, the heat exchanger was the component with the highest rate of exergy destruction.

Nomenclature

COP	Coefficient of performance
$c_{p,e}$	Constant pressure specific heat of exhaust gas [kJ/kg.K]
e^0_{ch,H_2O}	Water standard chemical exergy [kJ/kmol]
e^0_{ch,NH_3}	Ammonia standard chemical exergy [kJ/kmol]

h	Enthalpy [kJ/kg]
LHV	Low heating value [kJ/kg]
M	Molecular mass [kg/kmol]
$\dot{m}$	Mass flow rate [kg/s]
$\dot{Q}$	Heat transfer rate [kW]
$\dot{Q}_{cool}$	Thermal load from the evaporator [kW]
$\dot{Q}_{fuel}$	Heat supply by fuel [kW]
s	Specific entropy [kJ/kg.K]
T	Temperature [K]
$\dot{W}$	Power [kW]
$\dot{X}_{des}$	Exergy destruction [kW]
x	Mass fraction of ammonia

Greek Letters

ε	Exergy efficiency [%]
ψ	Exergy [kJ/kg]
η	Energy efficiency [%]

Subscripts

ac	Absorption chiller system
CCP	Combined cooling and power
e	Electric
H_2O	Water
i	Inlet
MT	Microturbine
NH_3	Ammonia
o	Outlet
0	Environment condition

Superscripts

Carnot	Carnot
ch	Chemical
$fuel$	Fuel
k	Component
ph	Physical

Acknowledgements

References

Ahrendts, J., 1980, "Reference States", *Energy,* Vol.5, pp. 667-677.

Dunn, P. D., Reay, D. A., 1997, *Heat Pipe*, Pergamon Press, 4th Edition.

Klein, S. A., Álvaro, F. L., 2003, EES-Engineering Equation Solver. Version 7.413-3D, F-Chart Software, Madson, WI.

Kotas, T. J., 1995, *The Exergy Method of Thermal Plant Analysis*, Krieger Publishing Company: Malabar.

Ibrahim, O. M., Klein, S. A., 1993, "Thermodynamic Properties of Ammonia-Water Mixtures," *ASHRAE Transactions* Paper CH-93-21.

Medrano, M., Mauzey, J., McDonell, V., Samuelsen, S. and Boer, D., 2006, "Theoretical Analysis of a Novel Integrated Energy System Formed by a Microturbine and an Exhaust Fired Single-Double Effect Absorption Chiller", *Int. J. of Thermodynamics*, Vol. 9, No.1, pp. 29-36.

Rossa, J. A. and Bazzo, E., 2006, "Thermodynamic Modeling and Second Law for an Ammonia-Water Absorption System Associated to a Microturbine", Proceedings of ECOS'2006 18th International Conference on Efficiency, Cost, Optimization, Simulation and Environmental Impact of Energy Systems - Aghia Pelagia, ISBN 960-87584-1-6, Vol 2, pp 651-658; Greece.

Peterson, G. P., 1994, *Heat Pipes Modeling, Testing and Applications*. John Wiley & Sons, New York.

Rucker, C. P. R., Bazzo, E. Jonsson M. R., Karlsson, S. J., 2003, "Exergy Analysis of a Compact Microturbine-Absorption Chiller Cogeneration System", Proceedings of COBEM 2003, São Paulo, Brazil.

Rucker, C. P. R., Bazzo, E., 2004, "Exergoeconomic Optimization of a Small Scale Cogeneration System using the Exergy Cost Theory". Proceedings of ECOS'2004 16th International Conference on Efficiency, Costs, Optimization, Simulation and Environmental Impact of Energy and Process Systems; ISBN-968-489-027-3, Vol. II, pp. 619-628; Guanajuato, vol. II, pp. 619-628.

Szargut, J., Morris, F. R., Steward, F. R., 1988, *Exergy Analisis of Thermal, Chemical, and Metalurgical Processes*, Hemisphere Publishing Corporation: New York.

Takeshita, K., Amano Y., Hashizume, T., 2005, "Experimental Study of advanced Cogeneration System with Ammonia-Water Mixture cycle at Bottoming", *Energy*, Vol.30, pp.247-260.